STRUCTURAL SCIENCE
CRYSTAL ENGINEERING
MATERIALS

Volume 78 (2022)

Supporting information for article:

Temperature-dependent crystal structure investigation of 4f hybridized thermoelectric clathrate Ba8–*x*Ce*x*Au*y*Si46–*y*

Jonas Sandemann, Hazel Reardon and Bo Brummerstedt Iversen

Table S1. The refined structural and FWHM parameters of $Ba_{7.74(9)}Ce_{0.26(9)}Au_{5.42(3)}Si_{40.58(3)}$ (space group $Pm\bar{3}n$) along with the obtained weight fractions of each of the three modelled phases. The displacement parameters are all given in units of 10^{-4} Å^2, the coordinates are fractional, and X as given by FullProf.

T (K)	a (Å)	U_{iso}^{2a}	U_{11}^{6d}	U_{22}^{6d}	U_{iso}^{6c}	U_{iso}^{16i}	U_{iso}^{24k}	x^{16i}	y^{24k}	z^{24k}	X	Weight fraction (%)		
												BCAS	$CeAu_2Si_2$	Si
120	10.39533(6)	52(3)	106(10)	120(5)	34(1)	37(7)	42(6)	0.1837(2)	0.1177(2)	0.3054(2)	0.147(1)	84.5(3)	8.9(1)	6.6(2)
205	10.39979(6)	70(3)	133(11)	155(6)	48(2)	53(8)	52(6)	0.1835(2)	0.1176(2)	0.3055(2)	0.148(1)	84.8(3)	8.8(1)	6.4(2)
300*	10.40680(6)	103(4)	183(13)	205(7)	64(2)	88(9)	96(8)	0.1835(2)	0.1178(2)	0.3053(2)	0.143(1)	85.0(3)	8.8(1)	6.3(2)
300†	10.40686(7)	88(3)	176(12)	195(7)	67(2)	58(8)	71(7)	0.1837(2)	0.1178(3)	0.3051(3)	0.149(1)	85.2(4)	9.3(1)	5.5(2)
387	10.41458(8)	113(4)	218(15)	248(9)	90(2)	88(10)	107(9)	0.1838(2)	0.1180(3)	0.3053(3)	0.142(1)	85.3(4)	9.3(1)	5.4(2)
485	10.42256(8)	132(5)	248(16)	283(9)	109(2)	97(11)	131(10)	0.1835(2)	0.1182(3)	0.3053(3)	0.140(1)	85.5(4)	9.1(1)	5.5(2)
587	10.43005(8)	152(5)	284(17)	318(10)	130(3)	117(11)	142(10)	0.1834(2)	0.1181(3)	0.3056(3)	0.139(1)	85.3(4)	9.2(1)	5.6(2)
686	10.43770(8)	170(5)	324(18)	349(10)	147(3)	122(11)	160(10)	0.1833(2)	0.1183(3)	0.3057(3)	0.134(1)	85.5(4)	9.1(1)	5.4(2)
784	10.44438(8)	188(5)	342(18)	388(10)	157(3)	140(11)	177(10)	0.1834(2)	0.1187(3)	0.3058(3)	0.137(1)	85.5(4)	9.4(1)	5.1(2)
881	10.4516(1)	208(6)	366(20)	419(12)	172(3)	163(13)	209(12)	0.1833(2)	0.1186(3)	0.3054(3)	0.138(1)	85.5(4)	9.4(1)	5.1(2)
977	10.4593(1)	228(6)	389(21)	436(12)	188(3)	179(13)	205(12)	0.1833(2)	0.1176(3)	0.3057(3)	0.147(1)	84.8(4)	9.8(1)	5.4(2)

*Low-temperature setup, †high-temperature setup

Table S2. The refined structural and FWHM parameters of the two identified impurity phases $CeAu_2Si_2$ (space group $I4/mmm$) and Si (space group $Fd\bar{3}m$). The displacement parameters are all given in units of 10^{-4} Å^2, the coordinate is fractional, and X as given by FullProf.

T (K)	$CeAu_2Si_2$							Si		
	a (Å)	c (Å)	U_{iso}^{Ce}	U_{iso}^{Au}	U_{iso}^{Si}	z^{Si}	X	a (Å)	U_{iso}	X
120	4.3112(1)	10.1963(2)	36(17)	30(8)	130(61)	0.392(2)	0.545(10)	5.4325(5)	59(15)	0.138(13)
205	4.3161(1)	10.1985(2)	57(18)	43(8)	144(63)	0.391(2)	0.531(10)	5.4324(5)	58(16)	0.131(13)
300*	4.3221(1)	10.2044(2)	55(21)	78(11)	243(83)	0.391(2)	0.536(11)	5.4335(6)	74(20)	0.082(15)
300†	4.3223(1)	10.2030(2)	57(18)	67(9)	156(64)	0.391(2)	0.519(9)	5.4333(5)	69(16)	0.120(13)
387	4.3282(1)	10.2091(2)	52(22)	93(11)	165(75)	0.392(2)	0.529(11)	5.4349(6)	69(20)	0.078(15)
485	4.3344(1)	10.2147(2)	66(22)	129(12)	148(74)	0.394(2)	0.476(10)	5.4361(6)	88(22)	0.068(14)
587	4.3399(1)	10.2197(2)	78(22)	151(12)	231(80)	0.395(2)	0.452(9)	5.4377(6)	115(23)	0.064(14)
686	4.3457(1)	10.2251(2)	92(23)	174(13)	213(76)	0.394(2)	0.424(9)	5.4391(5)	121(23)	0.056(14)
784	4.3506(1)	10.2301(2)	132(24)	185(13)	333(85)	0.394(2)	0.428(9)	5.4406(5)	115(23)	0.048(13)
881	4.3559(1)	10.2348(2)	151(27)	208(15)	316(90)	0.393(2)	0.400(9)	5.4421(5)	120(25)	0.043(15)
977	4.3616(1)	10.2399(2)	162(26)	244(15)	353(90)	0.390(2)	0.375(8)	5.4437(5)	132(25)	0.052(15)

*Low-temperature setup, †high-temperature setup

Table S3. Agreement factors from the refinements

T (K)	R_{Bragg} (%)			R_F (%)			R_{wp} (%)	χ^2
	BCAS	$CeAu_2Si_2$	Si	BCAS	$CeAu_2Si_2$	Si		
120	2.63	3.52	5.88	1.44	1.47	2.00	10.6	7.09
205	2.81	3.54	6.70	1.55	1.53	2.51	10.9	6.97
300*	2.75	3.37	6.10	1.71	1.71	2.21	10.9	6.55
300†	3.15	4.28	4.83	1.68	1.90	2.26	11.8	6.49
387	3.37	4.54	5.60	1.98	2.20	2.88	12.0	6.40
485	3.49	4.52	6.42	2.07	2.44	3.47	12.3	6.25
587	3.48	4.09	6.61	2.32	2.55	3.33	12.3	6.08
686	3.37	3.96	5.91	2.45	2.63	3.18	12.2	5.87
784	3.28	4.44	4.12	2.45	2.70	3.04	12.0	5.82
881	3.11	4.63	4.19	2.36	2.67	3.18	12.0	7.05
977	3.02	4.84	4.81	2.22	2.65	3.30	12.0	6.69

*Low-temperature setup, †high-temperature setup

Table S4. Temperature calibration of the N_2/hot air gas flow system

Set point (K)	Temperature (K)	Difference (K)
100	120	-20
200	205	-5
300	300	0
400	387	13
500	485	15
600	587	13
700	686	14
800	784	16
900	881	19
1000	977	33

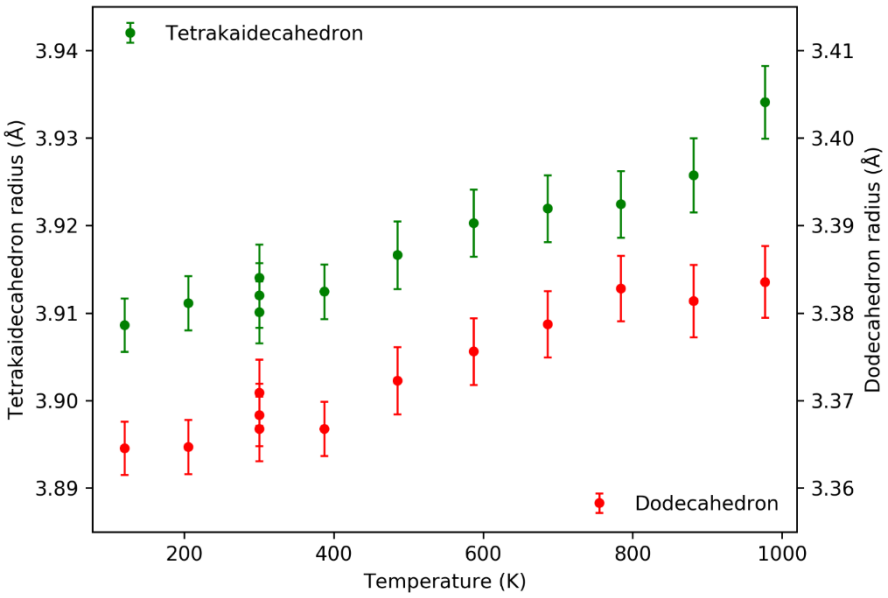

Figure S1. The radius of the tetrakaidecahedral- and dodecahedral cages calculated as the mean distance from the guest atom to host atoms of the corresponding cage.

The cage radii are calculated as the mean distance from the guest atom at the center to the host atoms comprising the corresponding cage

$$R_{\text{cage}} = a \times \frac{\sum_{j=1}^{N} \sqrt{\sum_{i=1}^{3} \left| X_i^{\text{guest}} - X_{j,i} \right|^2}}{N},$$

where a is the lattice parameter the outer sum runs over the different atoms in the cage N (20 in the dodecahedron and 24 in the tetrakaidecahedron), and the inner sum runs through the x, y, and z components of the guest- and host atom coordinate vectors, X^{guest} and X_j, respectively.

Table S5. The bond lengths in the host structure.

T (K)	24*k*-24*k* (Å)	6*c*-24*k* (Å)	16*i*-24*k* (Å)	16*i*-16*i* (Å)
100	2.447(3)	2.446(2)	2.391(2)	2.387(2)
200	2.446(3)	2.447(2)	2.392(3)	2.397(2)
300*	2.452(3)	2.449(2)	2.392(3)	2.396(2)
300†	2.452(4)	2.451(3)	2.392(4)	2.391(3)
400	2.458(4)	2.450(3)	2.394(4)	2.390(3)
500	2.464(4)	2.451(3)	2.394(4)	2.401(3)
600	2.464(4)	2.450(3)	2.398(4)	2.405(3)
700	2.472(4)	2.449(3)	2.398(4)	2.410(3)
800	2.479(4)	2.448(3)	2.400(4)	2.409(3)
900	2.479(4)	2.454(3)	2.399(4)	2.415(3)
1000	2.460(4)	2.459(3)	2.406(4)	2.417(3)

*Low-temperature setup, †high-temperature setup

Table S6. The bond lengths from the center of the tetrakaidecahedral cage (6*d* site) to the host atoms. There are two unique bond lengths to the 24*k* site, one roughly in the plane parallel to the hexagonal face (24$k_{\parallel}$) and one out of the plane (24$k_{\perp}$).

T (K)	6c (Å)	16i (Å)	24$k_{\parallel}$ (Å)	24$K_{\perp}$ (Å)
100	3.67531(3)	3.864(2)	4.016(3)	3.513(1)
200	3.67688(3)	3.867(2)	4.019(3)	3.514(1)
300*	3.67936(3)	3.869(2)	4.019(3)	3.518(2)
300†	3.67938(3)	3.869(2)	4.019(4)	3.519(3)
400	3.68211(3)	3.871(2)	4.020(4)	3.521(3)
500	3.68493(3)	3.876(3)	4.021(4)	3.525(3)
600	3.68758(3)	3.879(3)	4.025(4)	3.525(3)
700	3.69029(3)	3.882(2)	4.026(4)	3.528(3)
800	3.69265(3)	3.884(2)	4.025(4)	3.531(3)
900	3.69522(4)	3.887(3)	4.028(4)	3.536(3)
1000	3.69793(4)	3.890(3)	4.042(4)	3.533(3)

*Low-temperature setup, †high-temperature setup

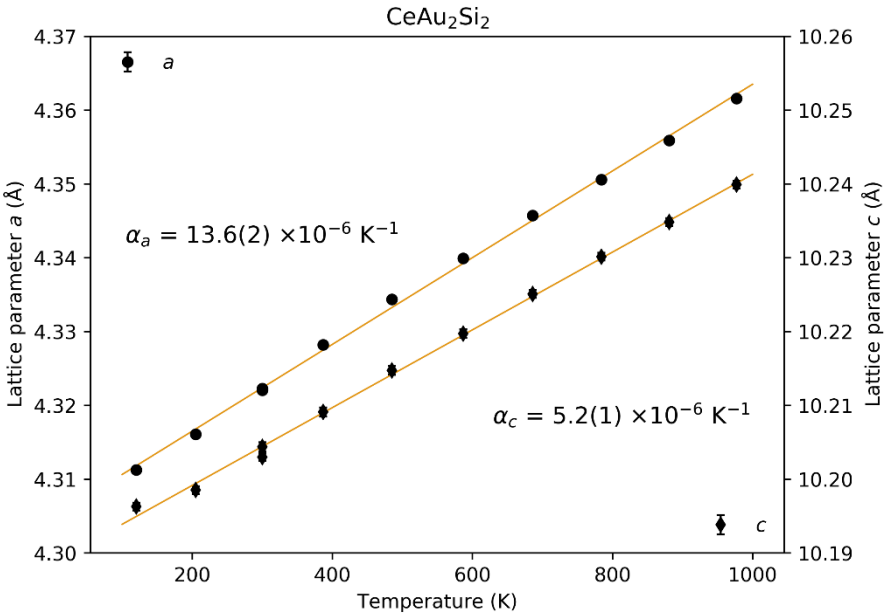

Figure S2. The lattice parameters of $CeAu_2Si_2$ as a function of temperature along with linear fits and the corresponding coefficients of linear thermal expansion.

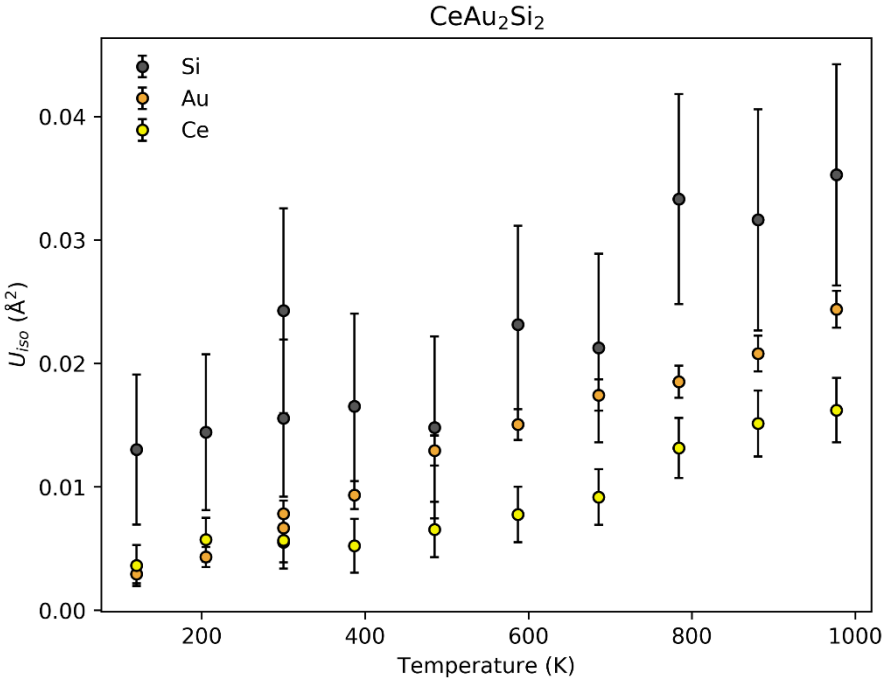

Figure S3. Isotropic mean square displacements in the $CeAu_2Si_2$ impurity phase as a function of temperature.

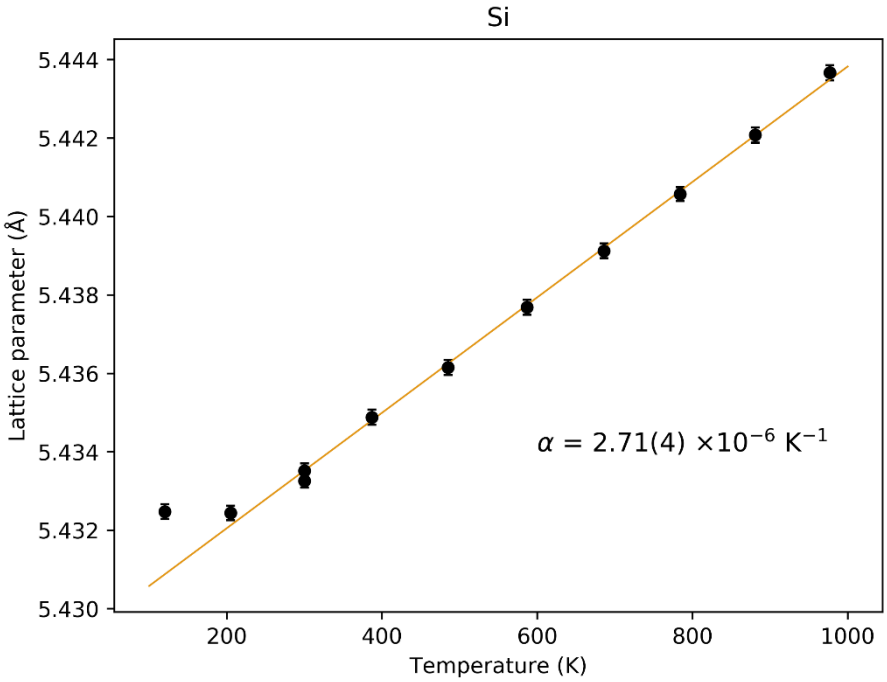

Figure S4. The lattice parameters of $CeAu_2Si_2$ as a function of temperature along with a linear fit and the corresponding coefficient of linear thermal expansion.

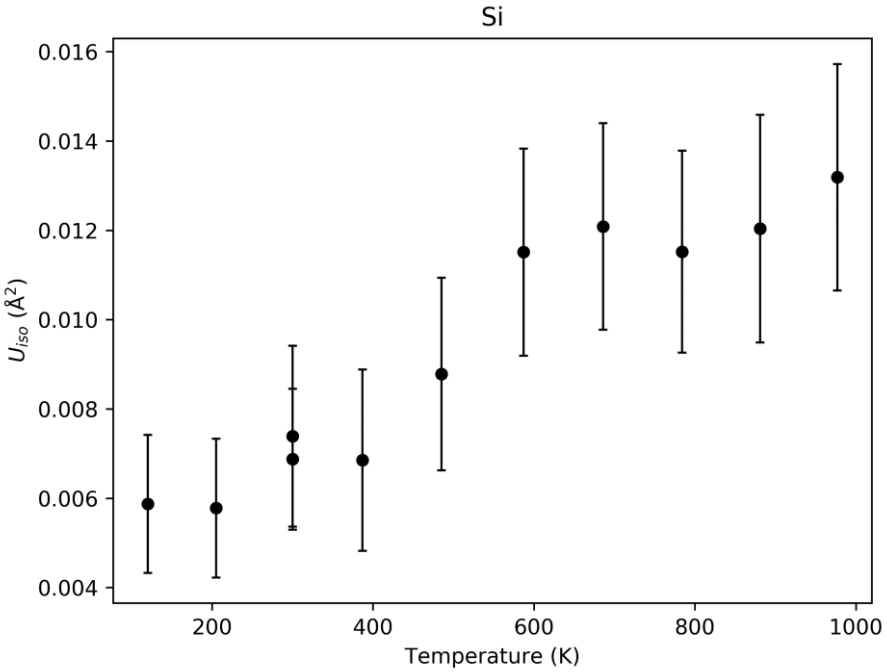

Figure S5. Isotropic mean square displacement in the Si impurity phase as a function of temperature.

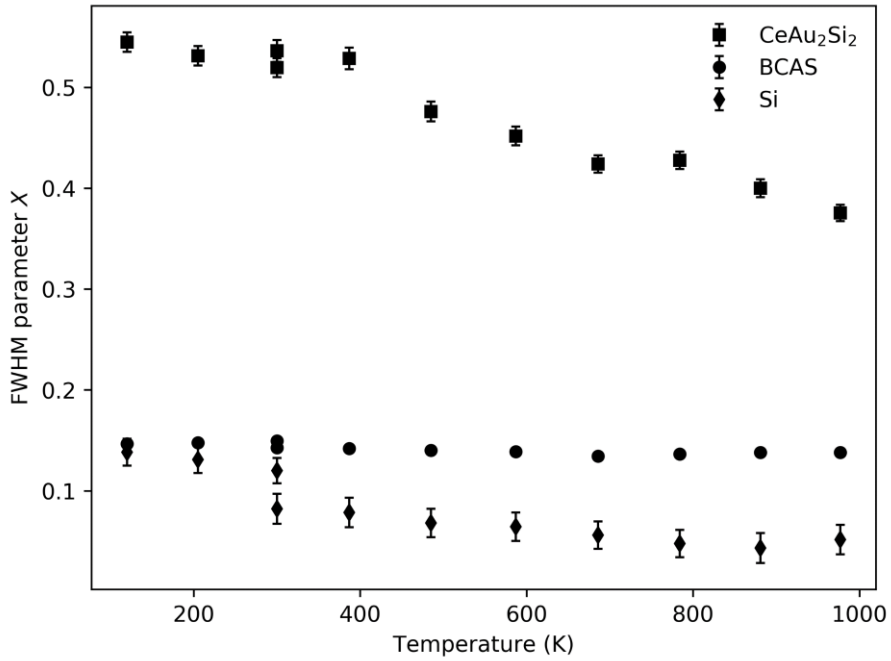

Figure S6. The Lorentzian FWHM parameter *X* as a function of temperature for the three modelled phases. It remains more or less constant for the main clathrate phase, whereas it decreases with temperature in the impurity phases.